Nano neuro knitting: Peptide nanofiber scaffold for brain repair and axon regeneration with functional return of vision

Rutledge G. Ellis-Behnke*†‡§, Yu-Xiang Liang†‡, Si-Wei You¶, David K. C. Tay†‡, Shuguang Zhang‖, Kwok-Fai So†‡§, and Gerald E. Schneider*

*Department of Brain and Cognitive Science and ‖Center for Biomedical Engineering, Massachusetts Institute of Technology, 77 Massachusett Avenue, Cambridge, MA 02139-4307; †Department of Anatomy, University of Hong Kong Li Ka Shing Faculty of Medicine and ‡State Key Laboratory of Brain and Cognitive Sciences, 21 Sassoon Road, Pokfulam, Hong Kong SAR, China; and ¶Institute for Neuroscience, Fourth Military Medical University, 17 Changle West Road, Xi'an 710032, People's Republic of China

Communicated by D. Carleton Gajdusek, Centre National de la Recherche Scientifique, Gif-sur-Yvette, France, January 23, 2006 (received for review November 9, 2005)

Nanotechnology is often associated with materials fabrication, microelectronics, and microfluidics. Until now, the use of nanotechnology and molecular self assembly in biomedicine to repair injured brain structures has not been explored. To achieve axonal regeneration after injury in the CNS, several formidable barriers must be overcome, such as scar tissue formation after tissue injury, gaps in nervous tissue formed during phagocytosis of dying cells after injury, and the failure of many adult neurons to initiate axonal extension. Using the mammalian visual system as a model, we report that a designed self-assembling peptide nanofiber scaffold creates a permissive environment for axons not only to regenerate through the site of an acute injury but also to knit the brain tissue together. In experiments using a severed optic tract in the hamster, we show that regenerated axons reconnect to target tissues with sufficient density to promote functional return of vision, as evidenced by visually elicited orienting behavior. The peptide nanofiber scaffold not only represents a previously undiscovered nanobiomedical technology for tissue repair and restoration but also raises the possibility of effective treatment of CNS and other tissue or organ trauma.

CNS regeneration | tissue repair | nanomedicine

There are several formidable barriers that must be overcome to achieve axonal regeneration after injury in the CNS, whether caused by a knife or a stroke. These obstacles are: (*i*) scar tissue formation after tissue injury (1–7); (*ii*) gaps in nervous tissue formed during phagocytosis of dying cells after injury (3, 8–14); (*iii*) factors that inhibit axon growth in the mature mammalian CNS (1, 3, 8–20); and (*iv*) failure of many adult neurons to initiate axonal extension (3, 8–12, 15, 17, 21, 22). In this paper, we describe the creation of a permissive environment for axonal regrowth using a synthetic biological nanomaterial that self assembles *in vivo*, with components that break down into beneficial building blocks and produce no adverse effects on the CNS. This discovery, by reducing or overcoming the first two obstacles and possibly more, allows for the reconnection of disconnected parts of the CNS after trauma.

Self-Assembling Peptide Nanofiber Scaffold (SAPNS)

The previously undiscovered treatment in this study used a designed self-assembling peptide (Fig. 1*a*) that spontaneously forms nanofibers (23–27), creating a scaffold-like tissue-bridging structure that we found to provide a framework for partial reinnervation by axons with regenerative potential in young and adult animals. Because the peptide fibers are nanoscale, there is likely a direct interaction between the peptide scaffold, the extracellular matrix, and the neural tissue on both sides of the lesion. These structures create a scaffold that connects the two faces of the lesion, allowing movement of cells into the scaffold. The peptide scaffold in our experiments created a permissive environment for axonal growth while discouraging or preventing the scar formation that normally occurs at an early stage. This material appears to offer a treatment for ameliorating or bypassing tissue disruptions after neuronal damage.

SAPNSs are synthetic biological materials formed through the assembly of ionic self-complementary peptides (23–30) and are designed by using alternating positive and negative L-amino acids that form highly hydrated scaffolds in the presence of physiological-concentration salts, i.e., saline, tissue culture media, physiological solutions, or human body fluids such as cerebrospinal fluid (23–25) (Fig. 1*b*). The scaffold consists of β-sheet ionic peptide containing 50% charged residues (23–25). A number of additional self-assembling peptides have been designed, synthesized, and characterized for salt-facilitated matrix formation (23–25). The SAPNS consists of interwoven nanofibers (Fig. 1*c*), and the individual fibers are $\approx$10 nm in diameter. The nanofiber density correlates with the concentration of peptide solution (27).

This designed peptide nanofiber scaffold provides several benefits over currently available polymer biomaterials: (*i*) The peptide scaffold forms a network of nanofibers that are similar in scale to the native extracellular matrix and therefore provides an "*in vivo*" environment for cell growth, migration, and differentiation (27); (*ii*) it can be broken down into natural L-amino acids and potentially used by the surrounding tissue, because the majority of the material is excreted in the urine (31); (*iii*) it is synthetic and free of chemical and biological contaminants that typically are present in animal-derived biomaterials such as many collagens (32); and (*iv*) it appears to be immunologically inert, thus avoiding the problem of neural tissue rejection. All of these attributes make it very attractive for using the peptide nanofiber scaffold in both *in vitro* and *in vivo* studies.

Our previous studies show that the SAPNS can support the attachment of a variety of mammalian primary cells in tissue culture (23–25). Additionally, one of the peptide scaffolds, arginine, alanine, aspartate, and alanine (RADA)16-I (Fig. 1*a*) supports not only the growth of PC12 cells (25) but also the formation of functional synapses *in vitro* using rat primary hippocampal neurons (25). Thus, RADA-I supports a wide range of neuronal growth and development using both *in vitro* and *in situ* cell culture systems.

Conflict of interest statement: No conflicts declared.

Freely available online through the PNAS open access option.

Abbreviations: SAPNS, self-assembling peptide nanofiber scaffold; SC, superior colliculus; RADA, arginine, alanine, aspartate, and alanine; P*n*, postnatal day *n*.

§To whom correspondence may be addressed. E-mail: rutledg@mit.edu or hrmaskf@hkucc.hku.hk.

www.pnas.org/cgi/doi/10.1073/pnas.0600559103

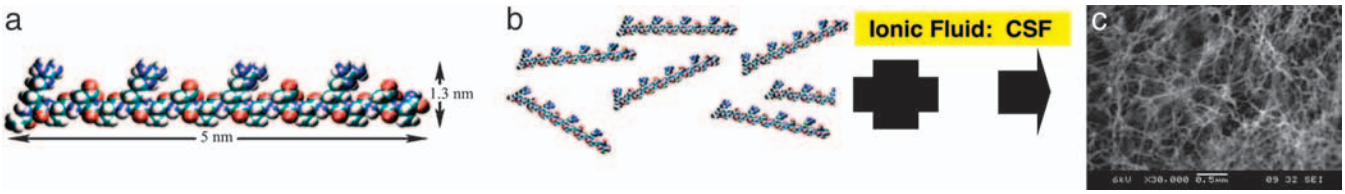

Fig. 1. SAPNS repair for the animal brain. (*a*) Molecular model of the RADA16-I molecular building block. (*b*) Molecular model of numerous RADA16-I molecules undergo self assembly to form well ordered nanofibers with the hydrophobic alanine sandwich inside and hydrophilic residues on the outside. (*c*) The SAPNS is examined by using scanning electron microscopy. (Scale bar, 500 nm.)

A tissue gap caused by deep transection of the optic tract in the hamster midbrain (Fig. 2 *a* and *b*) and injection of saline can completely block reinnervation of the superior colliculus (SC) by the retina even at young ages [postnatal days (P) 2–9] when the axons typically have more regenerative potential (33). Saline was used, because it is the standard irrigant for most neurosurgical procedures and is considered to be benign in the brain. Before the use of the SAPNS, we demonstrated substantial recovery of visual-orienting behavior in hamsters using a peripheral nerve optic tract bridge model (34).** In this model, the optic tract was completely severed at the brachium of the SC, and the reconnection of the optic tract was accomplished with several surgically implanted segments of sciatic nerve taken from one of the animals' legs (35).** However, the use of this model often results in leg disabilities in experimental animals (34, 35).**

In an attempt to facilitate optic tract regeneration with restoration of function, without additional clinical complications, we asked whether the SAPNS could create a permissive environment for regeneration in the damaged tissues as a substitute for sciatic nerve grafts. We examined both short- and long-term effects of injecting a peptide scaffold into the wound site in both young and adult animals using this model. (Fig. 2 *a* and *b*).

Here we report that the SAPNS not only permitted significant axonal growth through the site of the treated lesion, partially restoring the optic tract, but also resulted in the return of functional vision in brachium transected experimental adult animals. We show that use of this biological nanofiber scaffold (24, 25, 36) is an effective approach to facilitate the reconstruction of a continuous tissue substrate after CNS injury.

Results

Gap Closure and Healing in the Brain. In the first experiment, we applied 10 μl of the 1% SAPNS solution within the knife wound (1.5 mm deep and 2.0 mm wide) inflicted in the midbrain (in the rostral part of the SC) in P2 hamsters (37, 38). A schematic illustration of a parasagittal section of the dorsal midbrain of a hamster shows the location of the injury (Fig. 2*b*).

In all SAPNS-treated cases, the gap created in the tissue during injury was reduced in the first 24 h after surgery (Fig. 2*d*) and was reduced or completely eliminated at all later time points, 72 h (not shown), 30 days (Fig. 2*f*), and 60 days after surgery (Fig. 2 *g* and *h*). In the bright-field figure (Fig. 2*h*), tissue disruption is discernable only near the base of the cut (bottom arrow). In the dark-field photo (Fig. 2*g*), the cut area is indicated by arrows and shows healing that has become distorted over time because of development. The SAPNS appears to knit the tissue together. If the material was not optically transparent, it would be impossible to see the interface. We believe that this tight interface, coupled with the material's ability after self assembly to move with properties similar to those of the brain, serves to create a seamless junction between the tissue and the material. In contrast, the gap caused by the transection in the animals injected with 10 μl of saline remained visible by gross examination at all corresponding time points when examined at 24 h (Fig. 2*c*), 72 h, 30 days (Fig. 2*e*), and 60 days. When the tissue gaps in all lesioned animals are ranked and the treated experimentals are compared to the lesioned, saline-injected controls, there is no overlap. The rankings were made by three independent observers who did not know the group affiliations. The treatment effect was highly significant (Mann–Whitney U test, $n = 10$, 6, $U = 0$, $P < 0.001$).

Axons Regenerated Through the Treated Lesion. For anatomical evidence of axons regenerating through the lesion sites, we used a fluorescently tagged cholera-toxin subunit B (CT-B) fragment, which is taken up in retinal ganglion cells and transported to axon terminals. This tracer served as a marker of regeneration across wounds in the treated animals or regeneration failure in the lesioned controls. In preparation for axon tracing, the animals with postoperative survival times of 30, 45, 60, and 90 days received intraocular injections of 1 μl of 1% CT-B conjugated with FITC (List Biological Laboratories, Campbell, CA) into the vitreous humor of the eye, contralateral to the SC surgery site, 4 days before death (39, 40).

Axon tracing results for the young and adult treated animals in both experiments showed evidence of axonal growth into the SC caudal to the lesion site. The histological results revealed that 92% of the peptide scaffold-treated cases showed labeled regenerated axons in the SC. There were no labeled axons found in the SC in the lesioned control animals.

In the first experiment, with P2 operated animals, dense projections were observed to cross the SAPNS-treated lesion site and terminate in the SC (Fig. 3*b*). The innervation density in young animals (Fig. 3*c*) is 78% of that in a normal animal. In this example of innervation density (magnified from Fig. 3*b*), the white color represents axons, or axon terminals, labeled from the retina. In the untreated (but lesioned) control group, this injury resulted in the formation of a cavity, with no axonal regeneration (Fig. 3*a*). The scar response caused axons to form retraction bulbs and resulted in the arrest of growth. The resulting cavity that formed after the lesion in controls prevented the tissue from reconnecting between the faces of the lesion, except for a small tissue bridge above the tissue gap in some cases. The labeled axons (in light green) terminate rostral to the cut and were unable to regenerate across the lesion in all control animals.

In the second experiment, we used 8-week-old (young adult) animals. The optic tract was transected at the brachium of the SC (Fig. 4 *a* and *b*), and 30 μl of 1% SAPNS was injected into the injury site of the treated cases. We found, in all of these animals, a complete lack of gaps in the injured tissue and the appearance of "healed" tissue in all cases examined at 30, 45, or 90 days after injury. In the first set of lesioned controls, 30 μl of saline was injected into the wound site. Histological results revealed that, in all animals injected with 1% peptide scaffold solution and not in any of the controls, the tissue reconnected across the lesion at all time points (Mann–Whitney U test, $n = 12, 13$, $U = 0$, $P \ll 0.001$).

Schneider, G. E., You, S., So, K. F., Carter, D. A., Khan, F., Okobi, A. & Ellis-Behnke, R. (2000) *Soc. Neurosci. Abstr.* **26, 611.

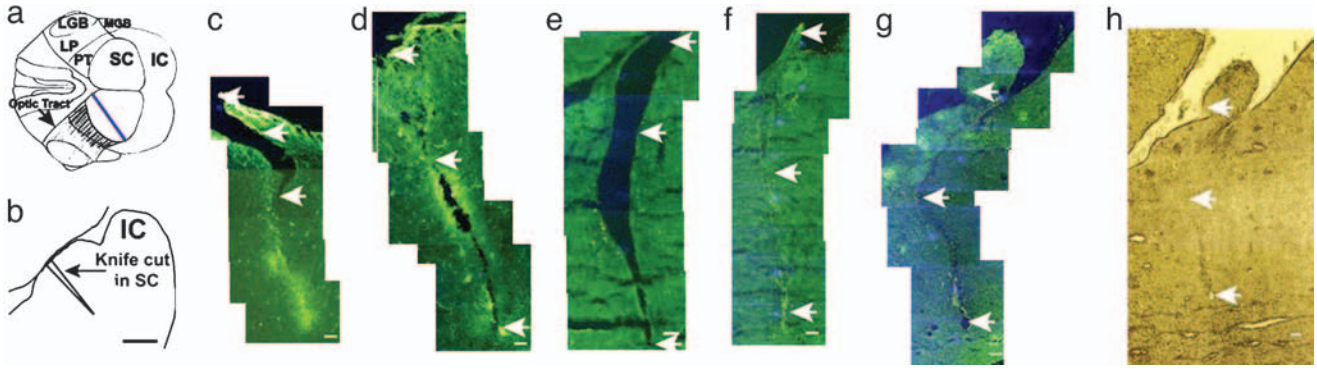

Fig. 2. SAPNS heals the brain in young animals. (*a*) Dorsal view reconstruction of the hamster brain with cortex removed. Rostral is to the left, and caudal is to the right. The blue line depicts the location of the optic tract transection made at P2 in the SC of the midbrain. Also shown: pretectal area (PT), lateral posterior nucleus (LP), medial geniculate body (MGB), lateral geniculate body (LGB), and inferior colliculus (IC). (*b*) Schematic illustration of a parasagittal section of the midbrain of a hamster, with the position and depth of the surgical knife cut indicated in the SC. Rostral is always to the left. Animals received an injection into the cut of 10 μl of saline in the controls or 10 μl of 1% SAPNS. The dark-field composite photos are parasagittal sections from animals 1, 30, and 60 days after lesion and treatment. Arrows indicate the path and extent of knife cut. Animals killed at 24 h after lesion and treatment: saline control animal (*c*) and SAPNS treatment (*d*). The treated case (*d*) has a very small gap, and the surface of the tissue has already started to reconnect both sides. (*e* and *f*) Thirty–day postlesion cases; *e* is a saline control, and *f* is an example of SAPNS-treated animals. Note the large gap in *e*. In the SAPNS treatment case (*f*), the gap is completely gone, and tissue has reconnected across the injury site. (*g*) Dark-field composite photo of a 60-day post-SAPNS solution-treated animal. (*h*) A corresponding bright-field picture. Note the lack of tissue disruption in the bright-field composite picture. All SAPNS solution-treated cases appear to have reconnected at the site of the lesion. [Scale bars, 500 μm (*b*); 100 μm (*c–h*).]

These adult cases showed results similar to the P2 operated animals at 30- and 60-day time points in Fig. 2. The lesions were healed in both young and adult animals. The two sides of the lesion came back together, and tissue appeared to be knitted together with little sign of the original lesion.

In the second experiment, with adult operated animals, axons have grown through the treated lesion site with an area of dense terminations in the SC in adults receiving the SAPNS solution (Fig. 4 *c–e*). In the best case, the SC was reinnervated to ≈82% of that of a normal animal (Fig. 4*g*). In addition, there are labeled fibers in the lower layers of the SC of regenerated axons closely resembling normal morphology. When comparing the SAPNS-treated cases with the lesioned saline-treated controls, we found that axons regenerated in the treated cases, and no axons regenerated in the controls (Fischer exact probability test, $P = 0.0000008$).

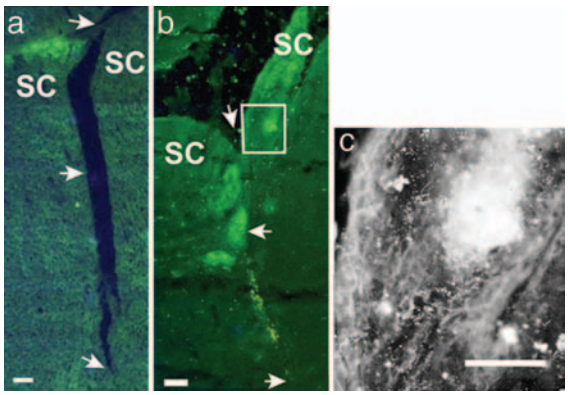

Fig. 3. SAPNS allows axons to regenerate through the lesion site in brain. The dark-field composite photos are parasagittal sections from animals 30 days after lesion and treatment. (*a*) Section from brain of 30-day-old hamster with 10 μl of saline injected in the lesion at P2. The cavity shows the failure of the tissue healing. The retinal projections, in light green at the top left edge of the cavity, have stopped and did not cross the lesion. Arrows indicate path and extent of knife cut. (*b*) A similar section from a 30-day-old hamster with a P2 lesion injected with 10 μl of 1% SAPNS. The site of the lesion has healed, and axons have grown through the treated area and reached the caudal part of the SC. Axons from the retina are indicated by light-green fluorescence. The boxed area is an area of dense termination of axons that have crossed the lesion. Arrows indicate path and extent of knife cut. (*c*) Enlarged view of boxed area in *b*. The regrown axons, shown in white, were traced with cholera-toxin fragment B labeling by using immunohistochemistry for amplification of the tracer. (Scale bars, 100 μm.)

We performed behavioral testing of the adult treated animals in experiment two for functional vision, as indicated by ability to orient toward a small object, and found that this visual ability had returned in 75% of these animals. The controls remained blind. We observed that the amount of axon reinnervation correlated with a return of functional vision in the SAPNS-treated adult animals (Spearman rank correlation, 0.91; $n = 8, P < 0.01$), with 75% of the animals demonstrating visually guided behavior (Fig. 5 *a–d*), although the animals' turning responses to the stimulus were 29% slower than responses by normal animals. The graph illustrates two very important points (Fig. 5*e*): (*i*) 75% of the treated animals responded well to the stimulus (in blue), whereas the lesioned controls (in yellow) spontaneously turn at a rate below 30%, which is consistent with a spontaneous response rate by blind animals. The data points represent the average of each week's behavioral testing for the animals. Two treated animals did not reach the minimum reinnervation density and responded the same as the blind controls; this was because of vascular injury during surgery, and 95% of the SC was gone. (*ii*) As testing progressed, the treated group's vision got better, and the responses became more robust, suggesting that, with sufficient reinnervation and long-term rehabilitation, this effect can be amplified. Tests of the pupillary response to light showed positive responses in all animals that also showed visual orienting and in only one animal without such orienting, but with a small amount of regeneration.

Discussion

Regenerated Axons Support Visual Behavior. We showed that the treatment with SAPNS solution enabled reconnection of brain tissue after acute injury that resulted in functional behavioral recovery. The scaffold knitted together tissue in the mammalian CNS in both young and adult animals. Before the SAPNS, no treatment we tried created a permissive environment for axonal regeneration that allowed growth through the center of a lesion. These experiments show that, with a single SAPNS solution

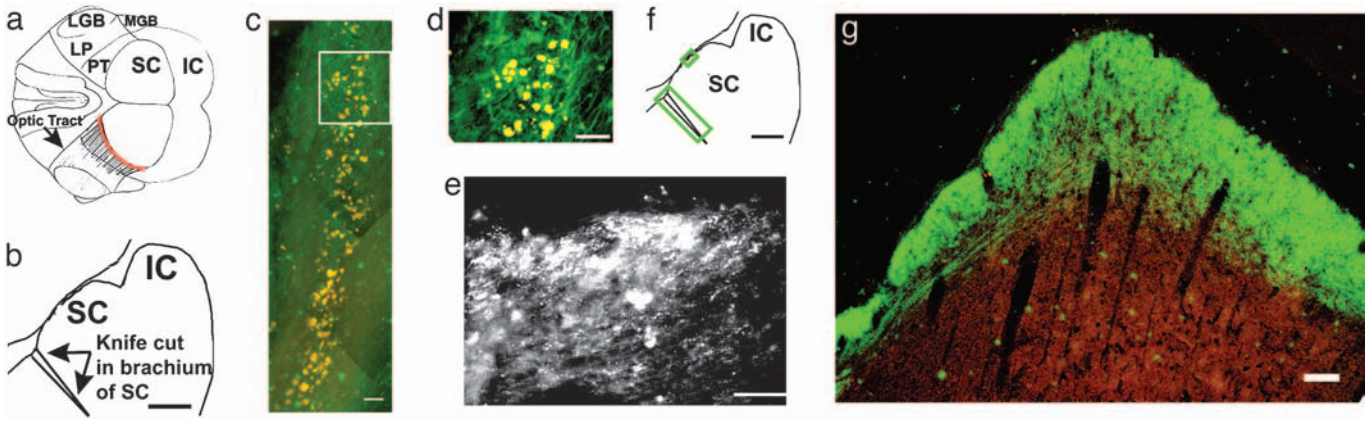

Fig. 4. Optic tract (OT) regenerated through lesion in adults. (*a*) Dorsal-view reconstruction of the hamster brain with cortex removed, as in Fig. 2*a*. Rostral is to the left, and caudal is to the right in all figures. The red line depicts the location of the OT transection at the brachium of the SC made at 8 weeks. (*b* and *f*) Schematic illustrations of parasagittal sections of the midbrain of a hamster, with the position and depth of the surgical knife cut indicated in the brachium of the SC. Animals received an injection of 30 μl of saline in the controls or 30 μl of 1% SAPNS solution. Two boxes in *f* show the locations of the dark-field pictures (*c* and *e*). (*c*) Dark-field photo of a parasagittal section from the brain of an 8-month old hamster treated with SAPNS at the time of surgery in the lesion site. The yellow dots show the location of the lesion. The axons, shown by green fluorescence, have grown through the site of lesion and are reinnervating the SC. Note the lack of tissue disruption. The boxed area is enlarged in *d*. Dense regenerated axons, in green, have grown through the lesion site. The yellow dots mark the location where the lesion was made and the area of subsequent treatment. (*e*) Dark-field picture from the superficial layers of SC caudal to the lesion, at a higher magnification; shown are regenerated axons and their dense terminals (in white). (*g*) Dark-field photo of a parasagittal section from the brain of an 8-month-old hamster treated with SAPNS at the time of surgery (at age 8 wk) in the lesion site. The axons, shown by green fluorescence, have grown through the site of lesion and are reinnervating the SC at ≈82% of normal density. Note the axon tracts in the deep layers of the SC. [Scale bars, 500 μm (*b* and *f*), 50 μm (*c*–*e*).]

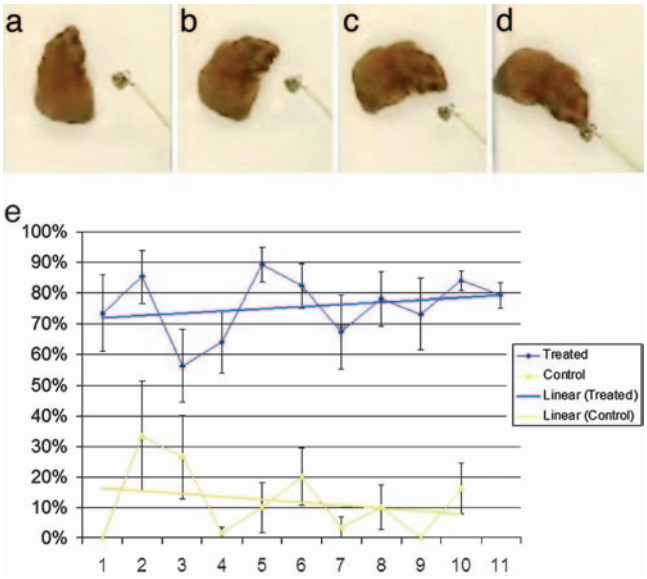

Fig. 5. Optic tract regeneration and functional return of vision. This SAPNS-treated adult animal turns toward the stimulus in the affected right visual field in small steps, prolonged here by movements of the stimulus away from the animal. Each frame is taken from a single turning movement, at times 0.00 (*a*), 0.27 (*b*), 0.53 (*c*), and 0.80 (*d*) sec from movement initiation. The animal reached the stimulus in the last frame. This is 29% slower than most turns by a normal animal. The recording was made 6 weeks after surgery and treatment when the animal started to show a response. See Movies 1 and 2, which are published as supporting information on the PNAS web site, for regenerated and control animals. (e) The graph shows the frequency (in percent) of response of all animals when a visual stimulus was presented to the eye connected to the treated optic tract (blue) or spontaneous turns of blind animals of the control group (yellow). The exceptions were the two animals that lost their SC after surgery; they were included in the average of the controls, because there was no difference in their response compared with the controls. On the *x* axis is the session number. Testing started 6 weeks after surgery (error bars SEM).

treatment at the site of injury, it is possible to overcome a major barrier to CNS regeneration in the optic tract of hamsters.

Our previous work using the optic tract transection peripheral nerve bridge model showed that a minimum level of 42% of normal local axonal innervation density in the target area is required for return of functional vision.** In two adult animals of the present study, one at 30- and another at 45-day survival, there was evidence of axons in the SC, but the innervation density reached <20% of normal density and, in agreement with the earlier study, failed to restore functional vision.

Because the SAPNS is highly hydrated, with ≈99% water content, it can fill an irregular void before assembly and then assemble to form the molecular nanofiber scaffold. This *in situ* self-assembly property may be critical, because most other materials do not conform to irregular voids created by injuries. This kind of intimate contact between nanofibers and the extracellular matrix may be critical to facilitate cell–scaffold interaction, thus encouraging brain injury healing. We have shown here that axons grew across the lesion site in 100% of the SAPNS-treated cases in both young and old animals, and that visually guided behavior was found in 75% of the adult animals receiving the SAPNS. The percentage would have been higher, except the vascular injury during surgery caused the SC to almost completely disappear in two adults. When the behavioral testing results for orienting are examined, there is a trend of improved responses as the testing progresses over time. This orienting behavioral result agrees with the results that Dunlop *et al.* (20) have reported for lizards.

The SAPNS is nontoxic, and the degradation products, L-amino acids, could potentially be used by nearby cells for growth and repair. Coupled with the ability of the material to facilitate neural tissue reconstruction within the first 24 hours after injury, peptide scaffolds offer a promising alternative to autografts of peripheral nerve or other tissues for recovery from CNS injury. We also found, in each case where the peptide scaffold solution was injected in the brain, that there was no apparent inflammatory response as seen in the control cases, which resulted in considerable cell death and a tissue gap. We have recently

learned that the material is broken down, and most of it is excreted in the urine in 3–4 weeks, depending on the volume of SAPNS solution used at 1% concentration (31). In addition, the spleen, brain, and lungs were checked by us for any molecular aggregations and evidence of blood clots at time points of 1, 2, 3, 5, 10, 30, 45, 60, and 90 days in both young and adult animals; none were found by using gross inspection as well as histological staining in the brain and lungs (preliminary data not shown here).

It is not clear exactly how the SAPNS promotes the closing of neural tissue gaps enabling axon regrowth. It is likely that it interacts at the nanoscale level with the extracellular matrix on both sides of the lesion. It is plausible that the SAPNS may promote cell migration into the lesion area, which creates a growth-permissive environment enabling axons to grow through the treated lesion site. It is also possible that it brings the two sides of the lesion together through a contractile process.

By using the designed SAPNS solution, we have facilitated CNS healing and have overcome some of the barriers to CNS axon regeneration previously thought to be nearly impenetrable. This allowed functional recovery demonstrated by a return of lost vision. Using nanobiomedical technology and molecular self assembly to repair brain structures opens up a new field and a new source of hope for efficacious treatment of CNS trauma. This successful outcome gives us a glimpse of what reconstructive brain surgery may hold for the future.

Materials and Methods

Young Animals. *In vivo* applications to brain wounds were carried out by using 53 P2 Syrian hamster pups, anesthetized with whole-body cooling. The scalp was opened, and the optic tract within the SC was completely severed with a deep knife wound through a slot cut in the cartilaginous skull, extending 1.5 mm below the surface, from the midline to a point beyond the lateral margin of SC (Fig. 2*a*). Animals were kept alive 24 h, 72 h, 30 days, and 60 days after surgery. During surgery, 10 animals were treated by injection into the brain wound of 10 μl of 1% SAPNS RADA16-I. Control animals with the same lesions included 6 injected with isotonic saline (10 μl), 27 earlier cases with knife cuts and no injection allowed to live 6–9 days, and 10 animals that were lesioned negative controls allowed to survive 24 h, 72 h, 30 days, and 60 days after the lesion.

Adult Animals. The 16 adult Syrian hamsters were anesthetized with an i.p. injection of sodium pentobarbital (50 mg/kg), then the animals were fitted in a head holder. The cortex was exposed and aspirated to reveal the rostral edge of the SC and the brachium of the SC on the left side. Each animal received a complete transection of the brachium of the SC (Fig. 3*a*). In many CNS regeneration models, the lesions are shallow. To make sure there would be no regeneration around the cut, our model used a 2-mm-deep cut. The increased depth prevented axons from growing around the bottom of the cut, ensuring that axons grew through the center of the lesion site rather than around it. In addition, special attention was paid to ensure there was complete transection of the brachium of the SC from the lateral edge to the midline. In the controls, there were no axons that grew through or around the 2-mm-deep lesion site.

With the aid of a sterile glass micropipette, 30 μl of 1% SAPNS solution was injected into the site of the lesion. The surgical opening in the skull was filled with saline-soaked gelfoam, and the overlying scalp was closed with wound clips. Animals were allowed to survive 30, 45, and 90 days from the date of surgery. Behavioral tests for visually guided orienting movements were performed on eight animals with 90-day survival times. Controls, all with lesions, consisted of 4 saline-treated controls and 27 brachium transections performed earlier, 7 with saline injections and 20 with no treatment. All were tested for behavior.

Animal Behavior Testing. All adult animals treated with the SAPNS were tested for visually elicited orienting movements. The animals that survived for 30 days were tested only three times before they were killed. The 45-day survival group was tested eight times. Data were not shown for either the 30- or 45-day groups, because (*i*) based on previous data, we did not expect to see any behavioral recovery before 6 weeks, and (*ii*) the data would artificially accentuate a training effect. Controls included normal animals and animals where one eye was removed to determine the rate of spontaneous turning toward the blind side. The group identity of an animal was unknown to the investigator during testing periods. To elicit orienting movements, sunflower seeds were first presented by hand and later with the aid of a white metal wire, on the end of which there was a small black rubber ball, slotted for holding a seed (Fig. 5 *a–d*). Animals, including nontreated and normal controls, were tested two to three times per week for a period of 90 days.** In both normal and blind animals, a turning response could also be elicited by touching the whiskers; therefore, care was taken to avoid whisker contact during visual presentations. Trials were video-recorded for analysis.

Independently, two investigators tested each animal for 10–20 min every other day or less frequently before any responses were seen in the affected field. On each test day, a minimum of 10 presentations were made on each side, with random choice of side. Visually elicited orienting movements were tested repeatedly by presenting a sunflower seed to part of the hamster's visual field (temporal or nasal, upper or lower), avoiding the nasalmost 45° (41). The stimulus was presented to the animal only when it had been waiting, relatively motionless, on the platform for several seconds. Left and right visual fields were tested, and all trials were videotaped with an overhead camera. A trial was not counted if the animal turned before the visual stimulus presentation commenced, or if the seed came into contact with the whiskers. A trial was counted if a response occurred within 2 sec of stimulus presentation. The completion of a turn was signaled by the animal's head coming to a stationary position within 5° of the stimulus for at least one-third of a second. Because an eye-enucleated animal generally failed to respond when the stimulus was placed outside the intact visual field, its whiskers were often touched on the blind side to elicit turns in that direction.

Preparation of the SAPNS Solution. The SAPNS solution was prepared by using RADA16-I dry powder (obtained from the laboratory of S.Z.) mixed in an Eppendorf tube. The solution contained 10 mg of RADA16-I powder in 1 ml of Milli-Q water (Millipore), mixed, then sonicated for 30 sec and filtered; this produced 1% SAPNS. We took extra care to ensure that the material was pure by mixing the powder into the liquid and letting it sit at room temperature for 1 month. An indication of its purity was that it remained clear and odorless.

Preparation for Tracing Regenerated Axons. Animals of the 30-, 45-, 60-, and 90-day survival groups were anesthetized with an i.p. injection of sodium pentobarbital (50 mg/kg). These animals received intraocular injections of 1 μl of 1% cholera-toxin subunit B conjugated with FITC into the vitreous humor of the right eye. This was accomplished with a glass micropipette (tip diameter, $\approx$10 μm) attached to a Pico Spritzer (General Valve, Fairfield, NJ) (39, 40). The subjects were then returned to their cages, under a heat lamp, and monitored until they recovered.

Four days after intraocular injection, the animals were killed with an overdose of anesthesia and perfused transcardially with 0.9% NaCl and 0.25% NaNO3 (pH 7.4), followed by 2%

paraformaldehyde in 0.1 M phosphate buffer (pH 7.4). The brains and eyes were removed and postfixed in 2% paraformaldehyde at 4°C for 4 days. For cryoprotection, we placed brains in 30% sucrose at 4°C until they sank. We cut 30-μm parasagittal sections on a cryostat, mounting them directly on gelatin-coated slides.

Immunolabeling of the Optic Tract Axons. The mounted sections were air-dried and then washed three times with PBS (pH 7.4) at 10-min intervals and preblocked in PBS (pH 7.4) containing 2% Triton 100, 2% normal rabbit serum, and 2.5% BSA for 30 min at room temperature. The slides were then incubated with goat anticholeragenoid (List Biological Laboratories) (1:8,000 dilution)/2% Triton 100/2% normal rabbit serum/2.5% BSA for 48 h at room temperature. Slides were again washed three times in PBS (pH 7.4) and incubated with fluorescent donkey anti-IgG antibodies Alexa-488 (secondary antibody from Invitrogen–Molecular Probes) (1:200 dilution) for 1.5 h at room temperature in a light-protected chamber. Slides were then washed four to five times in PBS (pH 7.4) at 5-min intervals and coverslipped with DAKO mounting slides (DAKO). The slides were visualized by using fluorescence microscopy, and pictures were taken with a Kodak DCS 520 digital camera. To reconstruct the locations of regenerated axons in the SC, serial sections were analyzed.

We gratefully acknowledge Dr. Peter Kook for his research support; Phillis Kau, technician in the Department of Anatomy at the University of Hong Kong Li Ka Shing Medical Faculty, for animal behavior, histology, and surgical assistance; and Dr. Ed Tehovnik, research scientist in the Brain and Cognitive Sciences Department at Massachusetts Institute of Technology, for his editing assistance. This work was supported by grants from the Whitaker Foundation and Deshpande Center of Massachusetts Institute of Technology, the Research Grant Council (RGC) of Hong Kong, and a donation from the late Mr. and Mrs. Ma Yip Seng. All protocols involving the use of live animals were approved by the Massachusetts Institute of Technology and the University of Hong Kong Committees on Animal Care.

1. Shearer, M. C. & Fawcett, J. W. (2001) *Cell Tissue Res.* **305,** 267–273.
2. Bradbury, E. J., Moon, L. D., Popat, R. J., King, V. R., Bennett, G. S., Patel, P. N., Fawcett, J. W. & McMahon, S. B. (2002) *Nature* **416,** 636–640.
3. Fawcett, J. W. & Asher, R. A. (1999) *Brain Res. Bull.* **49,** 377–391.
4. Rosenblat, G., Perelman, N., Katzir, E., Gal-Or, S., Jonas, A., Nimni, M. E., Sorgente, N. & Neeman, I. (1998) *Connect. Tissue Res.* **37,** 303–311.
5. Reinhardt, D., Mann, K., Nischt, R., Fox, J. W., Chu, M. L., Krieg, T. & Timpl, R. (1993) *J. Biol. Chem.* **268,** 10881–10887.
6. Lodish, H., Baltimore, D., Berk, A., Zipursky, S., Matsudaira, P. & Darnell, J. (1998) *Molecular Cell Biology* (Freeman, New York).
7. Huang-Lee, L. L., Wu, J. H. & Nimni, M. E. (1994) *J. Biomed. Mater. Res.* **28,** 123–132.
8. Fawcett, J. (1994) *J. Neurol.* **242,** S25–S28.
9. Gehrmann, J., Banati, R. B., Wiessner, C., Hossmann, K. A. & Kreutzberg, G. W. (1995) *Neuropathol. Appl. Neurobiol.* **21,** 277–289.
10. Nieto-Sampedro, M. (1999) *Adv. Exp. Med. Biol.* **468,** 207–224.
11. Norenberg, M. D. (1994) *J. Neuropathol. Exp. Neurol.* **53,** 213–220.
12. Streit, W. J., Walter, S. A. & Pennell, N. A. (1999) *Prog. Neurobiol.* **57,** 563–581.
13. Fisher, M. & Takano, K. (1995) *Baillieres Clin. Neurol.* **4,** 279–295.
14. McPhail, L. T., Stirling, D. P., Tetzlaff, W., Kwiecien, J. M. & Ramer, M. S. (2004) *Eur. J. Neurosci.* **20,** 1984–1994.
15. Chen, D. F. & Tonegawa, S. (1998) *Cell Death Differ.* **5,** 816–822.
16. Crespo-Santiago, D. (2004) *Rev. Neurol.* **38,** 843–851.
17. Stichel, C. C. & Muller, H. W. (1998) *Cell Tissue Res.* **294,** 1–9.
18. McPhail, L. T., McBride, C. B., McGraw, J., Steeves, J. D. & Tetzlaff, W. (2004) *Exp. Neurol.* **185,** 182–190.
19. Tetzlaff, W., Alexander, S. W., Miller, F. D. & Bisby, M. A. (1991) *J. Neurosci.* **11,** 2528–2544.
20. Dunlop, S. A., Tran, N., Tee, L. B., Papadimitriou, J. & Beazley, L. D. (2000) *J. Comp. Neurol.* **416,** 188–200.
21. Hirsch, S. & Bahr, M. (1999) *Adv. Exp. Med. Biol.* **468,** 199–205.
22. Choi, B. H. (1994) *Microsc. Res. Technol.* **28,** 193–203.
23. Zhang, S., Holmes, T., Lockshin, C. & Rich, A. (1993) *Proc. Natl. Acad. Sci. USA* **90,** 3334–3338.
24. Zhang, S., Holmes, T. C., DiPersio, C. M., Hynes, R. O., Su, X. & Rich, A. (1995) *Biomaterials* **16,** 1385–1393.
25. Holmes, T. C., de Lacalle, S., Su, X., Liu, G., Rich, A. & Zhang, S. (2000) *Proc. Natl. Acad. Sci. USA* **97,** 6728–6733.
26. Zhang, S., Marini, D. M., Hwang, W. & Santoso, S. (2002) *Curr. Opin. Chem. Biol.* **6,** 865–871.
27. Zhang, S. (2003) *Nat. Biotechnol.* **21,** 1171–1178.
28. Zubarev, E. R., Pralle, M. U., Li, L. & Stupp, S. I. (1999) *Science* **283,** 523–526.
29. Niece, K. L., Hartgerink, J. D., Donners, J. J. & Stupp, S. I. (2003) *J. Am. Chem. Soc.* **125,** 7146–7147.
30. Stupp, S. I., LeBonheur, V. V., Walker, K., Li, L. S., Huggins, K. E., Keser, M. & Amstutz, A. (1997) *Science* **276,** 384–389.
31. Buschow, K. H. J. (2001) *Encyclopedia of Materials: Science and Technology* (Elsevier, New York).
32. Lupi, O. (2002) *J. Am. Acad. Dermatol.* **46,** 790–793.
33. Cho, E. Y. & So, K. F. (1987) *Brain Res.* **419,** 369–374.
34. Sawai, H., Sugioka, M., Morigiwa, K., Sasaki, H., So, K. F. & Fukuda, Y. (1996) *Exp. Neurol.* **137,** 94–104.
35. Ellis-Behnke, R. G. (2002) Ph.D. dissertation (Massachusetts Institute of Technology, Cambridge, MA).
36. Zhang, S., Yan, L., Altman, M., Lassle, M., Nugent, H., Frankel, F., Lauffenburger, D. A., Whitesides, G. M. & Rich, A. (1999) *Biomaterials* **20,** 1213–1220.
37. Schneider, G. E. (1979) *Neuropsychologia* **17,** 557–583.
38. Schneider, G. E. (1973) *Brain Behav. Evol.* **8,** 73–109.
39. Ling, C., Schneider, G. E. & Jhaveri, S. (1998) *Visual Neurosci.* **15,** 559–579.
40. Mikkelsen, J. D. (1992) *Brain Res. Bull.* **28,** 619–623.
41. Schneider, G. E. (1967) *Psychol. Forsch.* **31,** 52–62.